Surface mediated ligands addressing bottleneck of room-temperature synthesized inorganic perovskite nanocrystals toward efficient light-emitting diodes

Dai, Jinfei; Xi, Jun; Zu, Yanqing; Li, Lu; Xu, Jie; Shi, Yifei; Liu, Xiaoyun; Fan, Qinhua; Zhang, Junjie; Wang, ShuangPeng

Published in:
Nano energy

DOI:
10.1016/j.nanoen.2020.104467

Publication date:
2020

Nano Energy 70 (2020) 104467

Contents lists available at ScienceDirect

Nano Energy

journal homepage: http://www.elsevier.com/locate/nanoen

Full paper

Surface mediated ligands addressing bottleneck of room-temperature synthesized inorganic perovskite nanocrystals toward efficient light-emitting diodes

Jinfei Dai [a], Jun Xi [b,c,**], Yanqing Zu [a], Lu Li [a], Jie Xu [a], Yifei Shi [a], Xiaoyun Liu [a], Qinhua Fan [e], Junjie Zhang [f], ShuangPeng Wang [g], Fang Yuan [a], Hua Dong [a], Bo Jiao [a], Xun Hou [a], Zhaoxin Wu [a,d,*]

[a] Key Laboratory of Photonics Technology for Information, Key Laboratory for Physical Electronics and Devices of the Ministry of Education, School of Electronic and Information Engineering, Xi'an Jiaotong University, Xi'an, 710049, China
[b] Global Frontier Center for Multiscale Energy Systems, Seoul National University, Seoul, 08826, South Korea
[c] Zernike Institute for Advanced Materials, University of Groningen, Nijenborgh 4, 9747 AG, Groningen, the Netherlands
[d] Collaborative Innovation Center of Extreme Optics, Shanxi University, Taiyuan, 030006, China
[e] Ningbo Exciton Innovation Materials Research Institute CO., LTD, Block 6A, Yunsheng Industrial Park 428 Mingzhu Road, Ningbo, 315040, China
[f] School of Chemical Science, Xi'an Jiaotong University, Xi'an, Shaanxi, 710049, China
[g] Joint Key Laboratory of the Ministry of Education, Institute of Applied Physics and Materials Engineering, University of Macau, Taipa, Macau, 999078, China

ARTICLE INFO

Keywords:
$CsPbBr_3$
Double-terminal ligand
Nanocrystals
Defect passivation
Light-emitting diodes

ABSTRACT

Cesium lead halide perovskites ($CsPbX_3$) have become superior candidates for perspective optoelectronic applications. However, room temperature synthesized $CsPbX_3$ nanocrystals (NCs) suffer from serious lattice/surface traps, mostly induced by nonequilibrium reactions and polar solvent systems. Thus, direct assembly of such poor crystals cannot be available toward high efficiency light emitting diodes (LEDs). To address this issue, differing from the general post-treatment works, here we propose a double-terminal diamine bromide salt to in situ passivate the surface traps of room temperature synthesized $CsPbBr_3$ NCs. High-quality NC solutions with photoluminescence quantum yield (PLQY) beyond 90% are obtained owing to the renovated surface bromide vacancies. Meanwhile, instead of longer oleylamine (OLA) ligand, the abridged diamine bromine ligand could significantly enhance charge transport throughout the NC film. In addition, the NC based LED performance is found related to chain length of the ligand, where the optimal luminance of 14021 Cd m^{-2} and current efficiency of 25.5 Cd A^{-1} are achieved by 1, 4-butanediamine bromide passivated NC devices. This work provides a direct efficient approach to meet the device application of room temperature synthesized perovskite NCs, underlines the significance of selective ligands to address the challenges of NC emitters in future displays and solid-state lighting.

1. Introduction

Cesium lead halide perovskite ($CsPbX_3$) nanocrystals (NCs) are considered as most promising materials for next-generation optoelectronic application due to their extraordinary properties [1–11], including high photoluminescence quantum yields (PLQY), high color purity and finely tunable emission spectrum [1,12,13]. In particular, such inorganic NCs, possessing high defect tolerance and high stability [14,15], can be readily synthesized in simplified protocols [16–19]. These comprehensive features endow $CsPbX_3$ NCs themselves as

* Corresponding author. Key Laboratory of Photonics Technology for Information, Key Laboratory for Physical Electronics and Devices of the Ministry of Education, School of Electronic and Information Engineering, Xi'an Jiaotong University, Xi'an, 710049, China.
** Corresponding author. Global Frontier Center for Multiscale Energy Systems, Seoul National University, Seoul, 08826, South Korea
E-mail addresses: daijinfei123@stu.xjtu.edu.cn (J. Dai), j.xi@rug.nl (J. Xi), 2667219182@QQ.com (Y. Zu), xjtulilu@mail.xjtu.edu.cn (L. Li), jiexu1991@stu.xjtu.edu.cn (J. Xu), syf1994@stu.xjtu.edu.cn (Y. Shi), liuxiaoyun@stu.xjtu.edu.cn (X. Liu), qinhua.fan@excitoniri.cn (Q. Fan), junjiezhang@mail.xjtu.edu.cn (J. Zhang), spwang@umac.mo (S. Wang), fang.y@stu.xjtu.edu.cn (F. Yuan), donghuaxjtu@mail.xjtu.edu.cn (H. Dong), bojiao@mail.xjtu.edu.cn (B. Jiao), houxun@opt.ac.cn (X. Hou), zhaoxinwu@mail.xjtu.edu.cn (Z. Wu).

https://doi.org/10.1016/j.nanoen.2020.104467
Received 26 September 2019; Received in revised form 3 January 2020; Accepted 3 January 2020
Available online 8 January 2020

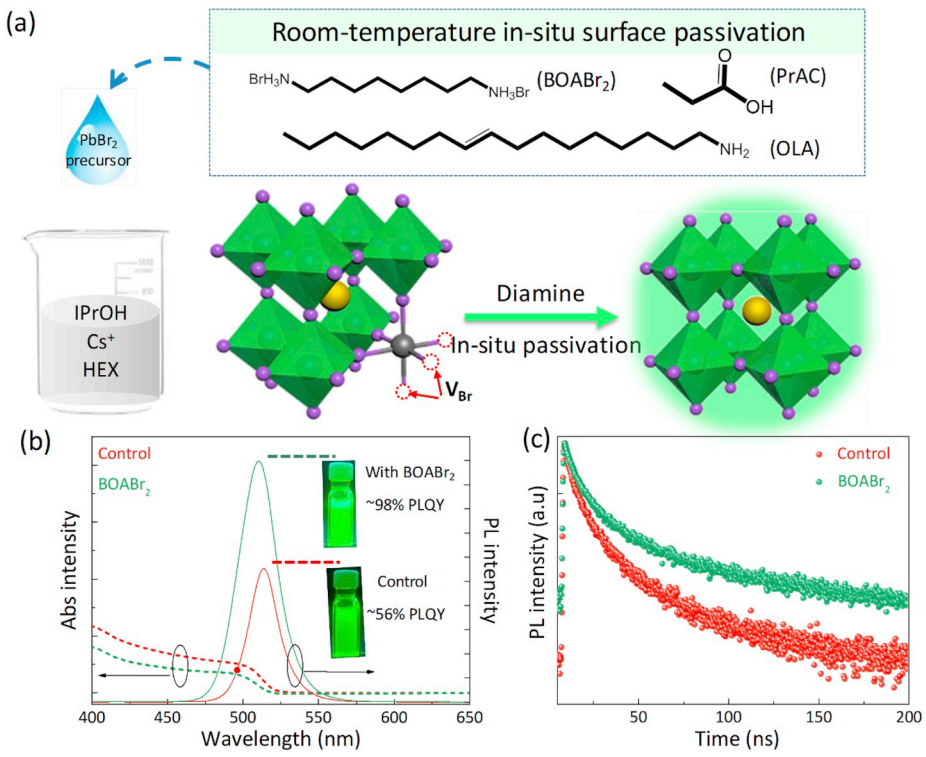

Fig. 1. (a) Schematic illustration of room temperature in situ surface passivation preparation process of $CsPbBr_3$ NC with diamine and surface changing after passivation. (b) UV–visible absorption spectra and steady-state PL spectra of Control- and $BOABr_2$-$CsPbBr_3$ NCs dispersed in octane solution. The insets are representative photograph of correspond NCs solution under 365 nm UV light and PLQY value. (d) Time-resolved PL of Control- and $BOABr_2$-$CsPbBr_3$ NCs solution measured at the PL peak ($\lambda = 510$).

attractive candidates of electroluminescence (EL) applications, especially light-emitting diodes (LEDs) [20,21].

In principle, PLQY and charge transport property of NC film dominate the efficiency of LED devices [16,22–27]. Generally, PLQY relies on precursor compositions, synthesis method and post-synthetic surface treatment [28–32], and transport property mostly depends on the ligands anchoring on NCs. In the past few years, considerable efforts have been dedicated to enhance the PLQY of these NCs [33–35], such as optimization of precursors (such as using L-type ligand in precursor, introducing zwitterionic ligand into precursor, adopting benzoyl halides as alternative precursors et al.) [28,36,37], imposing post-treatment with functional ligands or other chemical compounds (such as didodecyldimethylammonium bromide (DDAB) and $ZnBr_2$, 3-aminopropyltriethoxysilane (APTES) and HBr, potassium oleate, $PbBr_2$, NH_4SCN, ZnX_2, $NaBF_4$, NH_4BF_4 et al.) [24,31,38–47], and so on. However, near-unity PLQY in $CsPbX_3$ NCs is always achieved by hot-injection method, contradictory to the desirable low-cost consumption of practical application. Notably, a room temperature synthesis protocol of $CsPbX_3$ NCs endued with ultrahigh PLQY and superior charge transport property is urgent for highly efficient EL devices.

Currently, with respect to large scale room temperature synthesis protocols of $CsPbX_3$ NCs, Cs_2CO_3 and PbX_2 are the most popular raw materials [48,49], where PbX_2 itself simultaneously offer both lead and halide. According to the ionic reaction equation $2Cs^+ + 3PbX_2 = 2CsPbBr_3 + Pb^{2+}$, there should be uncoordinated lead ions occupied on the surfaces of the as-prepared perovskite NCs. Hence abundant halide vacancies defects aggregate and emerge on the non-stoichiometric NC surfaces. Besides, polar solvents, rather than nonpolar solvents, are involved within room temperature protocol, which can interact with lattices and lead to surface traps. As a result, these overall surface defects profoundly trap charge, limit PLQY enhancement, so as to hinder potential EL device application of $CsPbX_3$ NCs. Although post-synthesis surface treatment is maturely adopted to reduce such traps, subjected to the low-conductivity property of the typically indispensable long organic ligand molecules (like OLA), charge transport path in such NCs assembled films always be blocked, thus undermining EL device performance [32,41,47]. How to realize a win-win situation of promoting healing surface traps and charge transporting simultaneously is a vexing problem.

Here, we report a facile chemical method to in situ passivate surface traps of room temperature synthesized $CsPbBr_3$ NCs, that is, based on the control synthetic process a double-terminal diamine bromide ligand 1,8-octyldiamine bromide salt ($BOABr_2$) is used as an additional passivation material. The reason why we choose $BOABr_2$ can be ascribed to two aspects: 1) Excess bromide ions lead to equilibrium reactions on account of ideal Pb/Br stoichiometric ratio (1/3) in the reaction system, leading to offset surface bromide traps in the produced NCs. 2) Compared to OLA, the particular ligand $BOABr_2$ has shorter organic chain and two terminal ammonium (NH_3^+), which can shorter the charge transport path and assist charge transfer between the bridging crystals. Using this in situ passivation method, the fundamental optoelectronic properties (photoluminescence, carrier lifetime, and so on) of $CsPbBr_3$ NCs solution are obviously improved. Additionally, significantly enhanced charge (both holes and electrons) transport within the NC films has been observed, validated by the respective single-carrier devices. Furthermore, by optimizing the diamine bromide ligand chains, we achieved the best LED devices showing a maximum luminance of 14201 Cd m^{-2} and a current efficiency of 25.5 Cd A^{-1} based on 1, 4-butanediamine bromine ($BDABr_2$) passivated NCs. Such distinguished device performance suggests that our facile method can be eligible for the future application of room temperature synthesized perovskite NCs.

2. Results and discussion

$CsPbBr_3$ NCs colloidal solution in this work were prepared via a ligand-assisted reprecipitation (LARP) principle at room temperature in ambient air. In order to control the final size of $CsPbBr_3$ NCs, here, we used oleylamine (OLA) and propionic acid (Pr–Ac) as basic ligands (Fig. S1). With respect to the in situ passivated $CsPbBr_3$ NC preparation, additional diamine bromine salts (here take $BOABr_2$ as an example) were employed. Fig. 1a illustrates the synthesis process of $CsPbBr_3$ NC colloidal solution, whose details can be found in Experimental section.

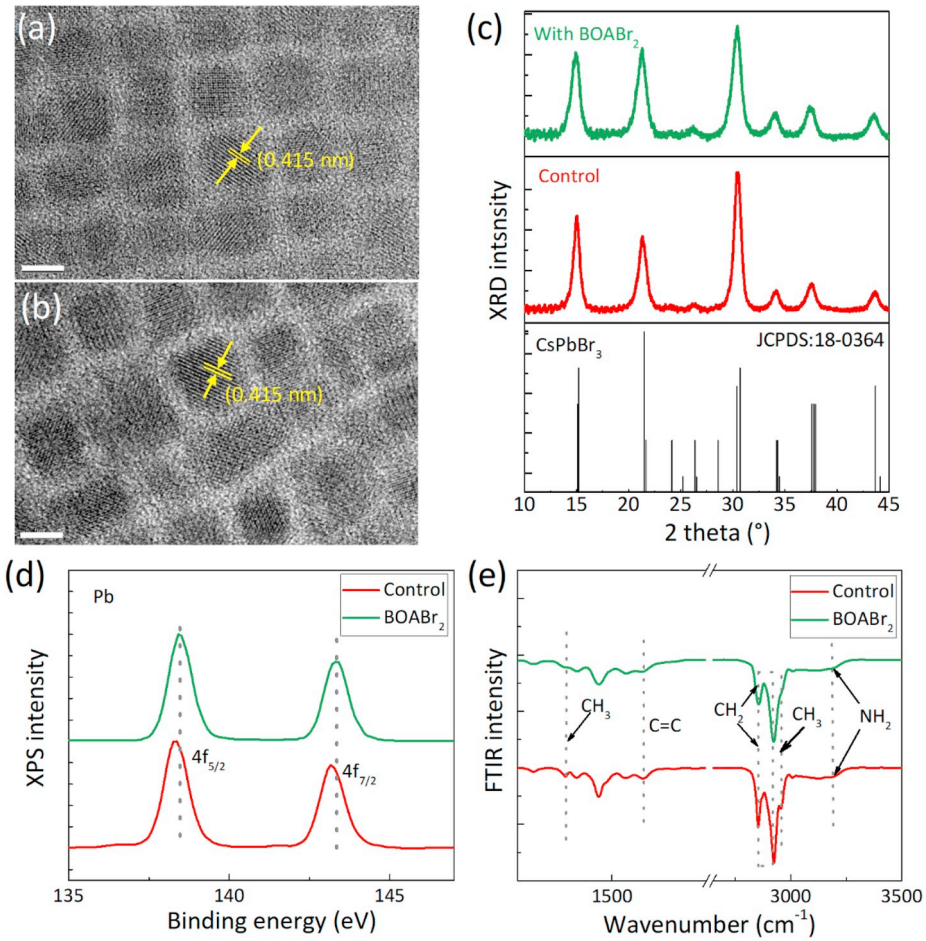

Fig. 2. Typical High resolution TEM image of (a) $BOABr_2$-$CsPbBr_3$ NCs, (b) Control-$CsPbBr_3$ NCs, with scale bar of 5 nm. (c) X-ray diffraction patterns of $BOABr_2$-and Conrtrol-$CsPbBr_3$ NCs films. (d) Pb 4f core level XPS spectra of $BOABr_2$-and Conrtrol-$CsPbBr_3$ NCs. The XPS spectra were calibrated using C 1s peak at 285.0 eV. e) FTIR spectra of $BOABr_2$-and Conrtrol-$CsPbBr_3$ NCs.

We can expect that with the addition of $BOABr_2$, the element compositions in precursors were adjusted from bromine deficient regime to relative bromine rich one, so that the surface traps can be suppressed.

Fig. 1b shows the UV–visible absorption spectra and steady-state PL spectra of Control- and $BOABr_2$-$CsPbBr_3$ NCs in octane solutions. Apparently, $BOABr_2$ passivated NC solutions show higher PL intensity and lower UV–visible absorption, revealing passivated traps compared to the control sample. PL variations dependent on polar solvent washing and timescales in Figs. S2 and S3 emphasize that our passivated NC colloidal solutions are much stable compared to the control one. PLQY (~98% vs ~56% in $BOABr_2$ and Control-NCs solution, respectively) obtained from an integrating sphere also demonstrates a much higher exciton radiative recombination of $BOABr_2$ NC solutions. Fig. S4 shows PLQY comparison of the thin films assembled from corresponding NCs, agreeing well with the results of their solution states. In addition, judging from time-resolved photoluminescence (TRPL) spectra, $BOABr_2$ based sample possessed longer average PL lifetime than the control one. The detail parameters used for fitting the PL decay in Control- and $BOABr_2$-$CsPbBr_3$ NC solutions are shown in Table S1. The overall results agree well with the possible reduced bromide vacancy traps, originating from more coordinated lead atoms offset by excess bromide anions from $BOABr_2$.

Afterwards, we investigated the $BOABr_2$ passivation effect on the structural properties of $CsPbBr_3$ NCs by high resolution transmission electron microscopy (HRTEM) and X-ray diffraction (XRD) measurements. As shown in Fig. 2a, irrespective of the samples, well defined cubic crystals with around 0.415 ± 0.015 nm inter-planar distance are observed, corresponding to (110) plane of the orthorhombic $CsPbBr_3$ lattice [46]. Besides, both XRD patterns (Fig. 1b) are consistent with that of the standard orthorhombic reference, proving that this passivation had little effect on the crystal phase structure. Intriguingly, X-ray photoelectron spectroscopy (XPS) spectra shows increased binding energy of Pb 4f and Br/Pb ratio of $BOABr_2$ passivated sample compared to the control one, confirming more coordinated lead species due to excess bromide contribution [42]. Then Fourier transform infrared (FTIR) spectra are conducted to understand the interactions between OLA/-$BOABr_2$ ligands and $CsPbBr_3$ NCs. Both samples show CH_2 and CH_3 symmetric and asymmetric stretching vibrations in the range of 2840–2950 cm^{-1}, which are the typical absorption bands for species with hydrocarbon groups. Notably, the passivated NCs own a C═C stretching vibration at 1585 cm^{-1} and a CH_3 vibration at ~1375 and ~2950 fade away, indicating that $BOABr_2$ is likely anchored to NC surfaces by partially substituting OLA (discuss later).

The morphologies and electronic properties of thin films assembled by $CsPbBr_3$ NC are critical to the performance of LED device. The SEM images of the films made from Control- and $BOABr_2$-$CsPbBr_3$ NCs are shown in Fig. 3a. It can be easily observed that the Control-$CsPbBr_3$ NC film displays obscure topography due to the poor conductivity of OLA ligand. By comparison, $BOABr_2$-$CsPbBr_3$ NC film demonstrates uniform and distinct nanocrystal morphology. According to the SEM images, we can deduce that ligand substitution of OLA with $BOABr_2$ occurred after passivation process. EDS elemental mapping of both films exhibit homogeneous lead and bromide distribution, from which we can also figure out increased Br/Pb ratio in $BOABr_2$-$CsPbBr_3$ NCs (Figs. S5 and

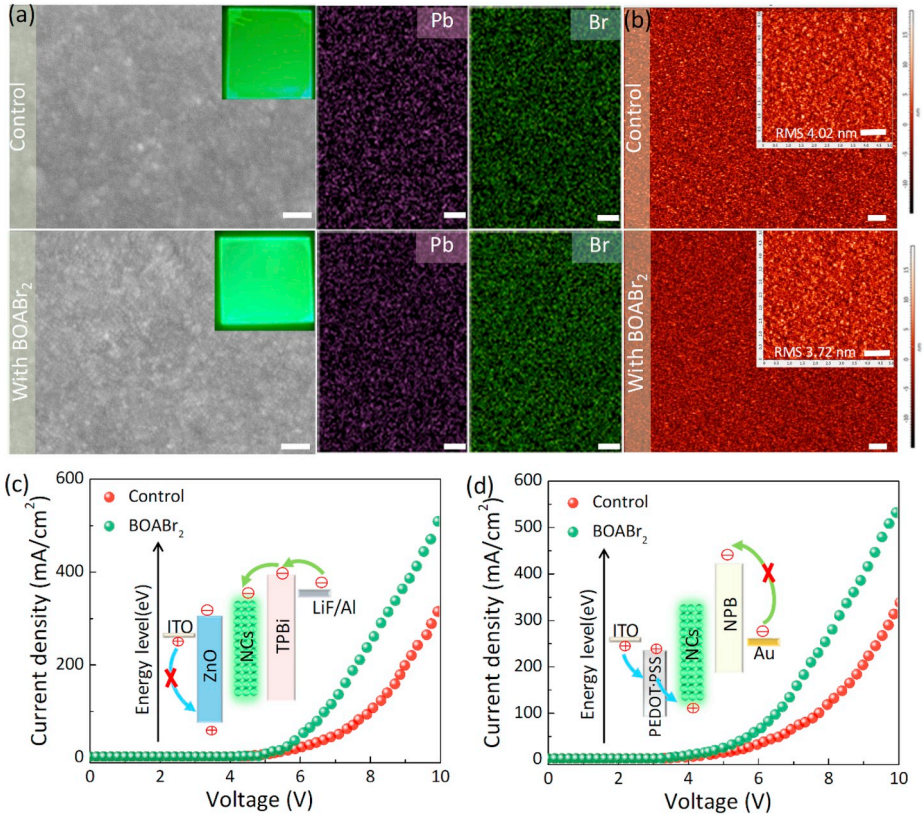

Fig. 3. (a) SEM images of Control-and $BOABr_2$-$CsPbBr_3$ NC film and the corresponding main element distribution (Pb and Br) in each film. (b) AFM surface images of Control- and $BOABr_2$-$CsPbBr_3$ NC film. Current density-voltage (J–V) characteristics of (c) electron-only and (d) hole-only LED device with Control- and $BOABr_2$-$CsPbBr_3$ NCs as active layer. Insets are schematic of corresponding device structure.

S6). In addition, the atomic force microscopy (AFM) topographic height images indicate uniformly distributed NC film with a lower root mean square (RMS) roughness of ~3.72 nm and 4.02 nm for the passivated and the control film, respectively. This similarity emphasizes that the ligand exchange does not change the film formation significantly. A little difference here likely originates from the different surface tension and vapor pressure of the coexisted organic ligands.

To further verify the hypothesis of ligand substitution mechanism induced by $BOABr_2$ addition, we tested and compared the current densities of hole-only and electron-only devices based on these two kinds of NCs films. Fig. 3c and d shows current-voltage (J-V) curves of electron-only and hole-only devices, respectively, whose configurations are shown as inserted images. Obviously, for both single carrier devices under identical condition, the current density of $BOABr_2$-NCs devices is higher than that of the Control-NCs, suggesting much improved charge transport property in $BOABr_2$ NC films. Theoretically, such phenomenon can be attributed to the shortened and ordered charge transport path between neighbor NCs in $BOABr_2$-NCs film, which is initiated by partial long chain OLA substituted by shorter and double-terminal $BOABr_2$.

All the aforementioned properties make the passivation approach assisted by the diamine bromide ligand as a promising way to achieve excellent room temperature synthesized $CsPbBr_3$ NC LED devices. To demonstrate the availability, a group of LED devices with a configuration of indium tin oxide (ITO) (120 nm)/poly(3,4-ethylenedioxythiophene)-poly(styrenesulfonate) (PEDOT:PSS) (~35 nm)/modified poly (bis(4-phenyl) (2,4,6-trimethylphenyl) amine) (M-PTAA) (~25 nm)/$CsPbBr_3$ NCs (~25 nm)/1,3,5-tris(1-phenyl-1H-benzimidazol-2-yl) benzene (TPBI) (40 nm)/LiF (1 nm)/Al (100 nm) were fabricated. Fig. 4a and b shows the cross sectional scanning electron microscope (SEM) images of the LED devices using $BOABr_2$-NC and Control-NC as well-defined active layer, respectively. The thicknesses of both $CsPbBr_3$ NCs films are estimated as 25 ± 5 nm according to cross sectional images, revealing a similar thickness of the two NC films. Besides, the energy-level alignments of the LED devices are shown as Fig. 4c. Then we turn our attention to the device performance based on different NC films. Compared to the Control-NCs device which can't turn on before 6.28 V, $BOABr_2$-NCs device exhibits greater current density, luminance and current efficiency (Fig. 4d and e) and reach the maximum luminance rapidly at a relative lower voltage. Especially, the peak luminance and maximum current efficiency could reach around 9200 Cd m^{-2} and 17.79 Cd A^{-1}, respectively, owing to the suppressed surface bromide vacancy traps as well as the enhanced charge transport induced by the diamine bromide ligand abridging the charge path, as summarized in Fig. 4f. In order to evaluate the device stability between $BOABr_2$-NCs and the Control-NCs, we have conducted the corresponding device electroluminance lifetime test, whose results are demonstrated in Fig. S7. Obviously, $BOABr_2$-NCs device is more stable than the control, implying enhanced NC stability benefiting from the unique double-terminal coordination ability of $BOABr_2$ ligands.

Furthermore, considering the above advantages of such double-terminal ligand, we attempted to continue promoting LED performance by shortening ligand chain. Here, other two ligands, 1, 4-butanediamine bromine ($BDABr_2$, abbreviated as C4) and 1, 2-ethylenediamine bromide ($BEABr_2$, abbreviated as C2) were adopted to replace $BOABr_2$. All the LED devices are built on the identical device structure as illustrated in Fig. 5a. The luminances, current density, current efficiencies and external quantum efficiencies (EQEs) of corresponding devices are summarized in Fig. 5b–d and Table S2. One can easily find that the device performance gradually increases as the ligand changes from $BEABr_2$ (C2), $BOABr_2$ (C8) to $BDABr_2$ (C4). The worst device performance from C2 passivation owes to the insufficient ligand exchange from OLA to C2 ligand under strong interaction between C2 and solvent molecules. Besides, C8 passivated device has improved but limited due to the insufficient conductivity of its long organic chains. Encouragingly,

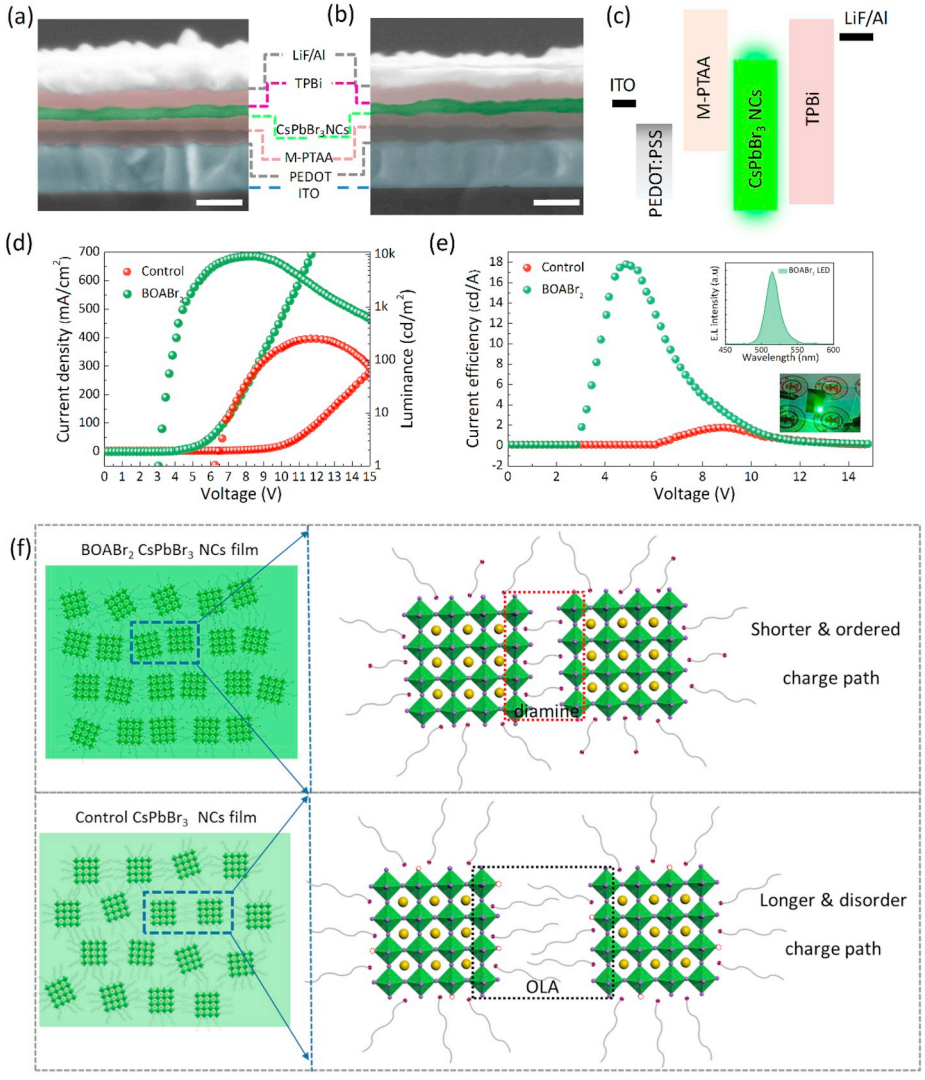

Fig. 4. SEM cross section image of LED device based on (a) $BOABr_2$-$CsPbBr_3$ NCs (b) Control-$CsPbBr_3$ NCs (scale bar:100 nm). (c) Energy-level diagram of LED devices with $CsPbBr_3$ NCs as emitting layer. (d) Current density (J) and Luminous intensity (L), (e) current efficiency (CE), as a function of driving voltage in $BOABr_2$-and Control-$CsPbBr_3$ NCs LEDs, respectively. The insets are EL spectra and a photograph of $BOABr_2$-device working at driving voltage of 5 V. (f) Illustration of the difference of charge transport path in $BOABr_2$-and Control-NC active emitting layer.

C4 passivated NCs device exhibited a maximum luminance of 14021 Cd m^{-1}, a current efficiency about 25.5 Cd A^{-1}, and an EQE of 8.56%, superior than those of C8 passivated NC LED device. This improvement can be easily understood due to further decreased charge transport path between nanocrystals capped with shorter alkyl chain ligand $BDABr_2$ (the detailed characterizations of $BDABr_2$ passivated NCs can be found in Fig. S8). Accordingly, the $CsPbBr_3$ NC LED device performance is related on the chain length of diamine, of which the best is achieved by the optimized ligand $BDABr_2$. Actually, the device maximum luminance and EQE results could be affected and varied by the device structure and effective area. Nevertheless, it can be easily found that our best result has joined the league of the state-of-art LED device performances based on low temperature $CsPbBr_3$ nanocrystals (Table S3).

3. Conclusion

In summary, an in situ surface passivation engineering strategy assisted by diamine bromine ligand was developed for room temperature synthesized $CsPbBr_3$ NCs. High-quality NC solutions are obtained by offset surface bromide vacancy traps, originating from equilibrium reactions on account of involved extra bromide anions. Besides, instead of traditional ligand, the shortened double terminal ligand leads to more compact NC film with significantly enhanced charge transport property. Using room temperature synthesized $CsPbBr_3$ NCs obtained via this in situ passivation approach, LED devices demonstrate a significantly enhanced performance compared to the control one. Optimizing the chain length of the double-terminal ligand, we achieved the best LED device with a maximum luminance (L) of 14021 Cd m^{-2} and a maximum current efficiency (CE) of 25.5 Cd A^{-1}, which is among the highest reported $CsPbBr_3$ NC LED leagues. The diamine bromide salt passivation strategy exploited for the room temperature synthesized inorganic perovskite NCs is believed to be qualified for future perovskite materials based displays and solid-state lighting.

4. Experimental section

Materials: Lead (II) bromide ($PbBr_2$, 99.9% trace metals basis), N, N-dimethylformamide (anhydrous, 99.8%), cesium carbonate (Cs_2CO_3, 99% purity), oleylamine (OLA, 80%–90% purity), 2-propanol (IPrOH, 99.5%), n-hexane (AR) n-propionic acid (PrAc, 99.5%) were used as received without any further purification. PTAA were purchased from Xi'an Polymer light Technology Corp. (China). TPBi (CC033, 99%, made in Taiwan, China), LiF (CC033, 99.99%, made in Taiwan, China) and NPB (99%, made in Taiwan, China) were purchased from Nichem. Aqueous dispersions of PEDOT: PSS (CLEVIOS PVP Al 4083) was obtained from Heraeus.

Synthesis of $BOABr_2$: Hydrobromic acid and 1,8-octyldiamine (BOA) were stirred in a 250 ml round bottom flask according to the molar ratio of 2.5:1 in an ice bath for 2 h. After stirring at 0 °C for 2 h, the resulting solution was evaporated by rotary evaporation at 65 °C and produced

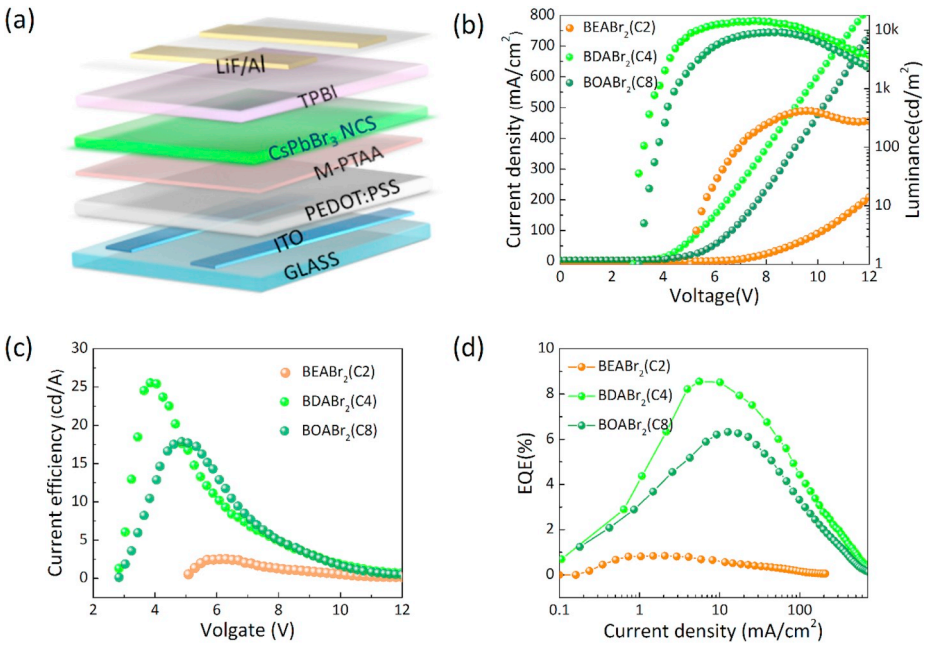

Fig. 5. Green LED device performance based on $CsPbBr_3$ NCs passivated with different diamine (varying chain length). (a) Schematic LED device structure. (b) Current density versus driving voltage (J–V) and luminance versus driving voltage (L–V) characteristics, (c) current efficiency versus driving voltage characteristics (CE-V), (d) external quantum efficiency (EQE) versus current density of corresponding devices.

synthesized solid $BOABr_2$. The solid product was washed several times with ethyl ether and then was dissolved in diethyl acetate, recrystallized from ethyl acetate several times. Then, the solid product was dried in vacuum at 60 °C for 24 h. Finally, the solid product $BOABr_2$ was obtained. The synthesis of $BDABr_2$ and $BEABr_2$ can following the same procedure only change BOA with BDA or BEA.

$CsPbBr_3$ nanocrystal synthesis: The synthesis of $CsPbBr_3$ NCs is a single-step injection method at room temperature and in air, overriding the traditional synthetic protocols that require inert conditions and high temperatures. For details of $CsPbBr_3$ NC colloidal preparation, 3 ml HEX, 3 ml IPrOH, and 10 μl ml Cs-PrAc (3.6 M Cs^+, Cs_2CO_3 dissolved in pure PrAc at room temperature) were mixed at room temperature and in air, forming a clear solution. Then 200 μl $PbBr_2$ precursor (0.375 mol $PbBr_2$ dissolved in 0.75 ml propionate (PAc), oleylamine (OLA) and N,N-dimethylformamide (DMF) mixed solvent with volume ration of 1:1:1, for $BOABr_2$ passivation sample DMF was substituted by $BOABr_2$ DMF solution) was injected swiftly, The solution immediately turned green, and then turned turbid within seconds. The $CsPbBr_3$ NCs were centrifuged for 5 min at 7000 r.p.m. and finally dispersed in 2 ml octane. A second centrifugation was performed after 72 h, at 3500 r.p.m for 5 min to discard any by-product, collecting supernatant we get the as-prepared NC colloidal.

Device fabrication: Firstly, ITO(15Ω/square)glass substrate was ultrasonic cleaning in ITO washing-up solution, ethanol, acetone, deionized water in sequence. After that, pretreated the ITO glass under ultraviolet and ozone for 5 min. For a hole-only device, PEDOT:PSS solution was spin-coated on treated ITO glass at 3000 rpm for 30 s and annealed at 120 °C for 20 min at ambient atmosphere. After that, $CsPbBr_3$ NCs film was deposited onto ITO/PEDOT:PSS substrate by layer by layer spinning coating at 2500 rpm and annealing at 100 °C for 10 min. After that, the substrate was transported to a thermal evaporation chamber, and then, electron blocking functional layer NPB and Au electrode were sequence deposited by thermal evaporation under high vacuum ($\sim 10^{-4}$ Pa) at depositing speed of 0.6 nm s^{-1}, 0.5 nm s^{-1}, respectively.

For the case of electron-only device, 30 nm ZnO electron transport layer was deposited onto a pretreated ITO substrate by spinning-coating ZnO sol-gel and followed by 30 min annealing at 180 °C, then spinning coating $CsPbBr_3$ NCs as mentioned in hole-only device fabrication process. Finally, hole-blocking layer TPBi and electrode LiF&Al were thermal evaporated at speed of 0.6 nm s^{-1}, 0.2 nm s^{-1}, 1.0 nm s^{-1}, respectively. For electroluminescence device, indium tin oxide (ITO)/PEDO: PSS/PTAA&PVK/$CsPbBr_3$ NCs/TPBi/LiF/Al device structure was used. Except the PTAA&PVK (M-PTAA) layer was spinning coating at 3000 rpm and annealing at 120 °C for 10 min, the else functional layer is fabricated by the same progress as mentioned in hole only or electron only device fabricating progress. Note, the emission area of the device is about 12 mm^2 as defined by the overlapping area of the ITO and Ag electrodes.

Characterization: Photoluminescence Quantum Yield and photoluminescence lifetime was tested using FLS920 spectrometer from Edinburgh Instruments. Transmission Electron microscopy (TEM) was carried out with a JEM-2100F TEM (JEOL Japan) operating at a beam energy of 200 keV. X-ray diffraction patterns were measured with a X-ray diffractometer (Shimadzu, XRD-6100) with Cu Ka radiation (λ = 1.54178 Å). X-ray photoelectron spectroscopy (XPS) spectra analysis was conducted by Bruker S8 Tiger. Fourier Transform infrared spectroscopy (FTIR) was recording using a Nicolet iS50 (TMO USA). The SEM image and EDS spectra were obtained by a field emission scanning electron microscope (Quanta 250, FEI, USA). The surface morphologies of the $CsPbBr_3$ NCs films were characterized by atom force microscopy (NT-MDT, Russia). The luminance (L) current density (J) voltages (V) characteristics were collected by a computer-controlled Keithley 2602 source and a calibrated silicon photodiode, in air. Electroluminescence spectra were measured using a PR650 spectrometer.

Author contributions

J.D., J.X. and Z.W. conceived and designed the experiments, J.D., Y. Z. and L.L. carried out experiments, including fabrication and analysis of the NCs and devices. Y.S. partially contributed to device structure design and test. J.X. (Jie Xu) and X.L. contribute to SEM analysis of device film and structure. Q.F. and J.Z. contribute to diamine bromine salts preparation and FTIR analysis. S.W. assist stability analysis. F.Y. contribute to partial TRPL measurement and analysis. J.B assisted with the using of LED device test system. J.X. together with J.D. co-wrote the manuscript.

H.D. improved the manuscript. All authors discussed the results and contributed to the final version of the paper. Z.W. and H.X. supervised the project.

Declaration of competing interest

The authors declare no competing financial interest.

Acknowledgment

This work was financially supported by National Natural Science Foundation of China (Grant No. 61875161, 11574248, and 61505161) and National Key R&D Program of China (Grant No. 2016YFB0400702). J. Xi acknowledges the Global Frontier R&D Program of the Center for Multiscale Energy System, South Korea (2012M3A6A7054855). The SEM and TEM work was done at International Center for Dielectric Research (ICDR), Xian Jiaotong University, Xi'an, China. The authors thank C. Ma and Y. Dai for their help in using TEM & SEM. We thank J. Liu and Y. Wang at Instrument Analysis Center of Xian Jiaotong University for their assistance of XPS and PLQY testing.

Appendix A. Supplementary data

Supplementary data to this article can be found online at https://doi.org/10.1016/j.nanoen.2020.104467.

References

[1] Q.A. Akkerman, V. D'Innocenzo, S. Accornero, A. Scarpellini, A. Petrozza, M. Prato, L. Manna, J. Am. Chem. Soc. 137 (2015) 10276.
[2] J. Liang, C. Wang, Y. Wang, Z. Xu, Z. Lu, Y. Ma, H. Zhu, Y. Hu, C. Xiao, X. Yi, G. Zhu, H. Lv, L. Ma, T. Chen, Z. Tie, Z. Jin, J. Liu, J. Am. Chem. Soc. 138 (2016) 15829.
[3] X. Li, Y. Wu, S. Zhang, B. Cai, Y. Gu, J. Song, H. Zeng, Adv. Funct. Mater. 26 (2016) 2435.
[4] P. Ramasamy, D.H. Lim, B. Kim, S.H. Lee, M.S. Lee, J.S. Lee, Chem. Commun. 52 (2016) 2067.
[5] J. Xi, C. Piao, J. Byeon, J. Yoon, Z. Wu, M. Choi, Adv. Energy Mater. 9 (2019) 1901787.
[6] M. Lu, Y. Zhang, S. Wang, J. Guo, W.W. Yu, A.L. Rogach, Adv. Funct. Mater. 29 (2019).
[7] L.N. Quan, B.P. Rand, R.H. Friend, S.G. Mhaisalkar, T.W. Lee, E.H. Sargent, Chem. Rev. (2019) 7444.
[8] J. Xi, K. Xi, A. Sadhanala, K.H.L. Zhang, G. Li, H. Dong, T. Lei, F. Yuan, C. Ran, B. Jiao, P.R. Coxon, C.J. Harris, X. Hou, R.V. Kumar, Z. Wu, Nano Energy 56 (2019) 741.
[9] H. Dong, J. Xi, L. Zuo, J. Li, Y. Yang, D. Wang, Y. Yu, L. Ma, C. Ran, W. Gao, B. Jiao, J. Xu, T. Lei, F. Wei, F. Yuan, L. Zhang, Y. Shi, X. Hou, Z. Wu, Adv. Funct. Mater. 29 (2019) 1808119.
[10] C. Zhang, B. Wang, W. Zheng, S. Huang, L. Kong, Z. Li, G. He, L. Li, Nano Energy 51 (2018) 358.
[11] X. Tang, Z. Hu, W. Chen, X. Xing, Z. Zang, W. Hu, J. Qiu, J. Du, Y. Leng, X. Jiang, L. Mai, Nano Energy 28 (2016) 462.
[12] Z. Yang, M. Wei, O. Voznyy, P. Todorovic, M. Liu, R. Quintero-Bermudez, P. Chen, J.Z. Fan, A.H. Proppe, L.N. Quan, G. Walters, H. Tan, J.W. Chang, U.S. Jeng, S. O. Kelley, E.H. Sargent, J. Am. Chem. Soc. 141 (2019) 8296.
[13] L. Protesescu, S. Yakunin, M.I. Bodnarchuk, F. Krieg, R. Caputo, C.H. Hendon, R. X. Yang, A. Walsh, M.V. Kovalenko, Nano Lett. 15 (2015) 3692.
[14] J. Kang, L.W. Wang, J. Phys. Chem. Lett. 8 (2017) 489.
[15] X. Zheng, Y. Hou, H.T. Sun, O.F. Mohammed, E.H. Sargent, O.M. Bakr, J. Phys. Chem. Lett. 10 (2019) 2629.
[16] J. De Roo, M. Ibanez, P. Geiregat, G. Nedelcu, W. Walravens, J. Maes, J.C. Martins, I. Van Driessche, M.V. Kovalenko, Z. Hens, ACS Nano 10 (2016) 2071.
[17] Q.A. Akkerman, M. Gandini, F. Di Stasio, P. Rastogi, F. Palazon, G. Bertoni, J. M. Ball, M. Prato, A. Petrozza, L. Manna, Nat. Energy 2 (2016) 16194.
[18] G. Almeida, L. Goldoni, Q. Akkerman, Z. Dang, A.H. Khan, S. Marras, I. Moreels, L. Manna, ACS Nano 12 (2018) 1704.
[19] D. Yang, Y. Zou, P. Li, Q. Liu, L. Wu, H. Hu, Y. Xu, B. Sun, Q. Zhang, S.-T. Lee, Nano Energy 47 (2018) 235.
[20] M. Chen, H. Hu, Y. Tan, N. Yao, Q. Zhong, B. Sun, M. Cao, Q. Zhang, Y. Yin, Nano Energy 53 (2018) 559.
[21] S. Peng, S. Wang, D. Zhao, X. Li, C. Liang, J. Xia, T. Zhang, G. Xing, Z. Tang, Small Methods 3 (2019) 1900196.
[22] J. Dai, J. Xi, L. Li, J. Zhao, Y. Shi, W. Zhang, C. Ran, B. Jiao, X. Hou, X. Duan, Z. Wu, Angew. Chem. Int. Ed. 57 (2018) 5754.
[23] J. Li, L. Xu, T. Wang, J. Song, J. Chen, J. Xue, Y. Dong, B. Cai, Q. Shan, B. Han, H. Zeng, Adv. Mater. 29 (2017).
[24] J. Song, T. Fang, J. Li, L. Xu, F. Zhang, B. Han, Q. Shan, H. Zeng, Adv. Mater. 30 (2018), e1805409.
[25] J. Pan, L.N. Quan, Y. Zhao, W. Peng, B. Murali, S.P. Sarmah, M. Yuan, L. Sinatra, N. M. Alyami, J. Liu, E. Yassitepe, Z. Yang, O. Voznyy, R. Comin, M.N. Hedhili, O. F. Mohammed, Z.H. Lu, D.H. Kim, E.H. Sargent, O.M. Bakr, Adv. Mater. 28 (2016) 8718.
[26] T. Chiba, Y. Hayashi, H. Ebe, K. Hoshi, J. Sato, S. Sato, Y.-J. Pu, S. Ohisa, J. Kido, Nat. Photonics 12 (2018) 681.
[27] J. Song, J. Li, X. Li, L. Xu, Y. Dong, H. Zeng, Adv. Mater. 27 (2015) 7162.
[28] A. Dutta, R.K. Behera, P. Pal, S. Baitalik, N. Pradhan, Angew. Chem. Int. Ed. 58 (2019) 5552.
[29] M. Imran, P. Ijaz, L. Goldoni, D. Maggioni, U. Petralanda, M. Prato, G. Almeida, I. Infante, L. Manna, ACS Energy Lett 4 (2019) 819.
[30] E. Moyen, H. Jun, H.M. Kim, J. Jang, ACS Appl. Mater. Interfaces 10 (2018) 42647.
[31] B.A. Koscher, J.K. Swabeck, N.D. Bronstein, A.P. Alivisatos, J. Am. Chem. Soc. 139 (2017) 6566.
[32] B.J. Bohn, Y. Tong, M. Gramlich, M.L. Lai, M. Doblinger, K. Wang, R.L.Z. Hoye, P. Muller-Buschbaum, S.D. Stranks, A.S. Urban, L. Polavarapu, J. Feldmann, Nano Lett. 18 (2018) 5231.
[33] G. Almeida, O.J. Ashton, L. Goldoni, D. Maggioni, U. Petralanda, N. Mishra, Q. A. Akkerman, I. Infante, H.J. Snaith, L. Manna, J. Am. Chem. Soc. 140 (2018) 14878.
[34] D. Quarta, M. Imran, A.L. Capodilupo, U. Petralanda, B. van Beek, F. De Angelis, L. Manna, I. Infante, L. De Trizio, C. Giansante, J. Phys. Chem. Lett. 10 (2019) 3715.
[35] S. Li, Z. Shi, F. Zhang, L. Wang, Z. Ma, D. Yang, Z. Yao, D. Wu, T.-T. Xu, Y. Tian, Y. Zhang, C. Shan, X.J. Li, Chem. Mater. 31 (2019) 3917.
[36] M. Imran, V. Caligiuri, M. Wang, L. Goldoni, M. Prato, R. Krahne, L. De Trizio, L. Manna, J. Am. Chem. Soc. 140 (2018) 2656.
[37] A. Pan, B. He, X. Fan, Z. Liu, J.J. Urban, A.P. Alivisatos, L. He, Y. Liu, ACS Nano 10 (2016) 7943.
[38] J. Pan, Y. Shang, J. Yin, M. De Bastiani, W. Peng, I. Dursun, L. Sinatra, A.M. El-Zohry, M.N. Hedhili, A.H. Emwas, O.F. Mohammed, Z. Ning, O.M. Bakr, J. Am. Chem. Soc. 140 (2018) 562.
[39] F. Krieg, S.T. Ochsenbein, S. Yakunin, S. Ten Brinck, P. Aellen, A. Suess, B. Clerc, D. Guggisberg, O. Nazarenko, Y. Shynkarenko, S. Kumar, C.J. Shih, I. Infante, M. V. Kovalenko, ACS Energy Lett 3 (2018) 641.
[40] S.A. Veldhuis, Y.K.E. Tay, A. Bruno, S.S.H. Dintakurti, S. Bhaumik, S.K. Muduli, M. Li, N. Mathews, T.C. Sum, S.G. Mhaisalkar, Nano Lett. 17 (2017) 7424.
[41] J.Y. Woo, Y. Kim, J. Bae, T.G. Kim, J.W. Kim, D.C. Lee, S. Jeong, Chem. Mater. 29 (2017) 7088.
[42] D. Yang, X. Li, Y. Wu, C. Wei, Z. Qin, C. Zhang, Z. Sun, Y. Li, Y. Wang, H. Zeng, Adv. Opt. Mater. 7 (2019).
[43] Y. Liu, F. Li, Q. Liu, Z. Xia, Chem. Mater. 30 (2018) 6922.
[44] T. Ahmed, S. Seth, A. Samanta, Chem. Mater. 30 (2018) 3633.
[45] V. González-Pedro, S.A. Veldhuis, R. Begum, M.J. Bañuls, A. Bruno, N. Mathews, S. Mhaisalkar, Á. Maquieira, ACS Energy Lett. 3 (2018) 1409.
[46] Q. Zhong, M. Cao, Y. Xu, P. Li, Y. Zhang, H. Hu, D. Yang, Y. Xu, L. Wang, Y. Li, X. Zhang, Q. Zhang, Nano Lett. 19 (2019) 4151.
[47] F. Di Stasio, S. Christodoulou, N. Huo, G. Konstantatos, Chem. Mater. 29 (2017) 7663.
[48] S. Sun, D. Yuan, Y. Xu, A. Wang, Z. Deng, ACS Nano 10 (2016) 3648.
[49] A. Swarnkar, R. Chulliyil, V.K. Ravi, M. Irfanullah, A. Chowdhury, A. Nag, Angew. Chem. Int. Ed. 54 (2015) 15424.